1 **The Role of Low Molecular Weight Fungal Metabolites in Grapevine Trunk**
2 **Disease Pathogenesis: Eutypa Dieback and Esca**
3

4 **Gabriel Perez-Gonzalez[1], Dana Sebestyen[1], Elsa Petit[2], Jody Jellison[3] Laura Mugnai[4], Eric**
5 **Gelhaye[5], Norman Lee[6], Sibylle Farine[7], Christophe Bertsch[7], Barry Goodell[1*]**
6

7 [1]Department of Microbiology, University of Massachusetts, Amherst, MA 01003, U.S.A
8 [2] Stockbridge School of Agriculture, University of Massachusetts, Amherst, MA 01003, U.S.A
9 [3] Center for Agriculture, Food and the Environment, University of Massachusetts, Amherst, MA
10 01003 U.S.A.
11 [4]Department of Agricultural, Food, Environmental and Forestry Science and Technology,
12 University of Florence, Firenze 50144, Italy
13 [5]Université de Lorraine, INRAE, Interactions Arbres-Microorganismes, F-54000 Nancy, France
14 [6]Chemical Instrumentation Center (CIC), Boston University, Boston, MA 02215, U.S.A
15 [7]Laboratoire Vigne Biotechnologies et Environnement EA-3991. Université de Haute-Alsace,
16 Colmar 68008, France
17
18 [*]Corresponding author: Barry Goodell; Email: bgoodell@umass.edu
19

20 **ABSTRACT** Eutypa dieback and Esca are serious grapevine trunk diseases (GTDs) caused by fungal

21 consortia causing large economic losses in vineyards. Depending on the disease the species

22 involved include *Eutypa lata*, *Phaeoacremonium minimum*, and *Phaeomoniella chlamydospora*.

23 There is a need to understand the complex pathogenesis mechanisms used by these causative

24 fungi to develop treatments for the diseases they cause. Low molecular weight metabolites

25 (LMW) are known to be involved in non-enzymatic oxygen radical generation in fungal

26 degradation of wood by some Basidiomycota species, and as part of our work to explore the basis

27 for fungal consortia pathogenesis, LMW metabolite involvement by the causal GTD fungi was

28 explored. The GTD fungal pathogens examined, *Eutypa lata*, *Phaeoacremonium minimum* and

29 *Phaeomoniella chlamydospora*, were found to produce low molecular weight iron binding

30 metabolites that preferentially reduced iron or redox cycled to produce hydrogen peroxide.

31 Uniquely, different LMW metabolites isolated from the GTD fungi promoted distinct chemistries

1

32    that are important in a type of non-enzymatic catalysis known as chelator-mediated Fenton

33    (CMF) reactions. CMF chemistry promoted by LMW metabolites from these fungi allowed for the

34    generation of highly reactive hydroxyl radicals under conditions promoted by the fungi. We

35    hypothesize that this new reported mechanism may help to explain the necrosis of woody

36    grapevine tissue as a causal mechanism important in pathogenesis in these two grapevine trunk

37    diseases.

38

39    **IMPORTANCE** Understanding the pathogenesis of grape trunk diseases (GTDs) is the key to the

40    development of disease control and treatment. While fungal extracellular enzyme systems are

41    typically cited relative to their fungal mechanisms in pathogenesis, non-enzymatic mechanisms

42    have been less studied in this regard and the role of low molecular weight (LMW) fungal

43    metabolites in GTD development is quite limited. In this article, we demonstrate that GTD-

44    causative fungal pathogens *Eutypa lata*, *Phaeoacremonium minimum* and *Phaeomoniella*

45    *chlamydospore* produce LMW phenolic metabolites under iron-restricted conditions. These

46    metabolites undergo a series of redox reactions, with different fungi producing metabolites that

47    preferentially either reduce iron, or generate hydrogen peroxide, under conditions simulating

48    grapevine woody tissue. These conditions have the potential to promote generation of highly

49    damaging hydroxyl radicals through a mechanism that appears to be similar to non-enzymatic

50    chelator-mediated Fenton (CMF) chemistry which is involved in fungal degradation of wood by

51    non-related fungal orders. This is the first report of CMF chemistry promoted by GTD-causative

52    fungi under laboratory conditions and the research suggests an alternate pathway that may

53    contribute to pathogenesis in GTDs, and a potential target for vine protection.

54

57

## INTRODUCTION

59

60 Grapevine trunk diseases (GTDs) are caused by a complex of fungi that were described as early

61 as the end of the 20th century. Most GTD fungi attack the perennial tissues of the grapevine and

62 ultimately lead to the death of the plant (1-3) and are characterized by the dieback and

63 necrosis/decay of the stem tissue. Some of these diseases can show foliar symptoms that may

64 not appear until deterioration of the stem wood is advanced (4). Although Eutypa dieback has

65 been reported to be caused solely by *Eutypa lata* or other *Eutypa* species, current literature

66 suggests that these pathogens are also associated with other GTDs. Further, *Eutypa* spp. is often

67 associated with a consortium of other fungi, especially the Diaporthales order, with

68 *Phaeoacremonium minimum* (Pmin) and *Phaeomoniella chlamydospora* (Pch) predominating (5-

69 8). Eutypa dieback, Esca, and *Botryosphaeria* dieback are the most significant GTDs involving one

70 or several xylem-inhabiting fungi, with Pch and Pmin typically found in consortia for Esca disease

71 development (3, 9).

72

73 Most GTD fungal pathogens enter grapevine trunk wood in vineyards through pruning wounds,

74 inhabiting the xylem cells in the woody tissue and causing, with time, significant necrosis and

75 decay, ultimately leading in some of those diseases to foliar symptoms and cordon and vine death

76 (4). In Eutypa dieback, as the disease progresses complete loss of yield, stunting of shoots, and/or

3

77    loss of cordons and vines occurs, with older vineyards experiencing as much as 30% necrosis of

78    cordons or vines. In the USA, Eutypa dieback and *Botryosphaeria* dieback predominate in

79    California and have also been an emerging issue for cold-climate vineyards in the Northeastern

80    US and in British Colombia, Canada. In California alone, losses by GTDs each year amount to 14%

81    of the value of the wine grapes produced with economic loss of more than $260 million per year

82    (10, 11). GTDs also cause up to 2 billion in losses to vineyards globally each year (12).

83

84    While the pathogenic mechanisms and foliar damage in Eutypa dieback has been reported to be

85    associated with the production of eutypine and other phytotoxic compounds (13), the

86    mechanisms involved in producing woody tissue necrosis and other symptoms associated with

87    both Eutypa dieback and Esca are still not well understood. Importantly, it is also unknown why

88    a consortium of fungi is typically involved in both diseases (13, 14).

89

90    Wood decay by brown rot Basidiomycota species is similar in some respects to the necrosis in

91    grapevine wood caused by Ascomycota GTD fungi. Decay initiated by brown rot fungi produces

92    a type of wood degradation where both holocellulose and lignin are depolymerized by a highly

93    oxidative non-enzymatic chelator mediated Fenton (CMF) mechanism (15-21). After, or

94    concurrent with CMF action, the polysaccharide component of the wood cells is then

95    preferentially extracted from the wood via the action of fungal extracellular carbohydrate active

96    enzymes (CAZymes), while the lignin component is repolymerized within the wood cell wall (19,

97    22). In *E. lata*-infected grape wood, structural glucose and xylose from the hemicellulose are also

98    preferentially degraded and depleted from the wood while lignin is degraded much more slowly

99   (23) similarly to brown rot wood decay. The residual lignin in both brown rotted wood and in

100   necrotic wood attacked by GTD fungi is brown in coloration because of the residual or modified

101   lignin which remains. Because of the similarities to brown-rot wood decay, and prior reports on

102   the action of oxygen radical generation in Esca disease (24) , we considered that a mechanism

103   similar to CMF chemistry might potentially play a role in GTD fungal attack of grapevine wood.

104   The hallmark of the CMF system is the production of fungal low molecular weight (LMW)

105   compounds that promote the mediated Fenton reaction (eq. 1) by the reduction of $Fe^{3+}$ to $Fe^{2+}$

106   with the wood cell wall, and away from the fungal hyphae (15, 19). This CMF chemistry is

107   promoted by a reduction in pH of the fungal micro-environment (typically to pH 5.5 or lower).

108   Brown rot fungi generally reduce the pH of their micro-environments to approximately pH 4 or

109   lower, and this is thought to aid in promoting a sequence of reactions leading up to the Fenton

110   reaction occurring within the wood cell wall (19, 25, 26). In the low pH environment of the brown

111   rot fungal extracellular matrix (ECM) which immediately surrounds the fungal hyphae, the pH is

112   lower than pH 4.0 and iron will be sequestered (19). However, within the wood cell wall the pH

113   is maintained at approximately 5.5, and at that pH LMW compounds will redox cycle with iron to

114   generate $Fe^{2+}$ and also generate $H_2O_2$ (27, 28). Both of these reactants are required for the

115   generation of hydroxyl radicals (HO•), which are required to be generated within the cell wall for

116   oxidative depolymerization of both cellulose and lignin to occur. This action then leads to further

117   cell wall deconstruction by fungal CAZymes (22, 29).

118

119 $$Fe^{2+} + H_2O_2 \xrightarrow{pH\,3-5.5} Fe^{3+} + OH^- + OH^{\cdot} \qquad\qquad (eq.\,1)$$

120

5
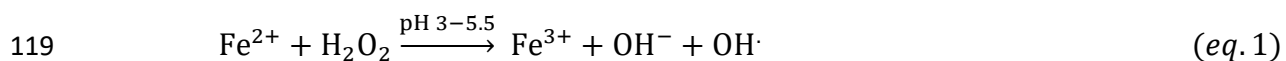
121    Osti and DiMarco reported that fungal supernatants of Pch and Pmin contained phenolate

122    siderophore-like compounds, and their analysis suggested that catecholate compounds from the

123    fungal supernatants were present that could also reduce iron, generate hydroxyl radicals (HO$^\bullet$)

124    and depolymerize cellulose (24). However, their supernatants also contained high molecular

125    weight components such as extracellular enzymes which could have skewed some of their

126    results. Therefore, in our research we assessed only the ultrafiltered <5kDa fraction of LMW

127    metabolites. We did not assess for siderophore receptor sites on the fungal membranes as

128    examination of classic siderophore function was not part of our objectives for this research.

129    *Eutypa lata* (Elata) and other fungal species involved in GTDs are known to produce acetylenic

130    phenols and heterocyclic analogues similar to some types of siderophores (30, 31), and several

131    LMW phenolic metabolites have been identified from Pmin and Pch (32). But it has not been

132    reported whether these compounds have the ability to redox cycle or reduce iron as has been

133    observed with some types of catecholate compounds produced by brown rot decay fungi, such

134    as 2,5-dimethoxyhydroquinone (2,5-dimethoxybenzoquinone) (15).

135

136    Our research examines the nature of LMW compounds produced by Elata, Pmin and Pch, and by

137    combinations of these three fungi, specifically for iron reduction and hydroxyl radical generation

138    to determine if there is a link between the LMW metabolites produced and non-enzymatic

139    chemistries that may produce hydroxyl radicals in a manner similar to that which has been

140    demonstrated in CMF chemistry with other wood degrading fungi.   We hypothesize that

141    chemistries similar to the CMF mechanism, and enhanced by LMW metabolites produced by

6

142    these fungi, could potentially play a key role in the initial stages of Eutypa dieback and Esca

143    disease, particularly associated with wood grapevine tissue necrosis.

144

145    **MATERIALS AND METHODS**

146

147    The three fungi involved in the Eutypa dieback consortia used in our current work were

148    *Phaeomoniella chlamydospora* (Pch, isolate UCD7872), *Phaeoacremonium minimum* (Pmin,

149    isolate UCD7770), and *Eutypa lata* (Elata, isolate UCD7746); all isolated from vineyards in Lodi,

150    California. These fungi were grown both in single culture and in combination (Elata_Pch;

151    Elata_Pmin; Pmin_Pch) for six-weeks in low-iron media. LMW iron-binding metabolite

152    production was assessed, as was hydroxyl radical generation. All analysis were done in triplicate

153    unless otherwise stated.

154

155    **Culture media.** Iron-free cultures with restricted nutrient media were used to promote

156    biosynthesis of iron-binding LMW compounds (33), with all glassware acid washed in 10% HCl for

157    24 hours, rinsed with deionized distilled water (ddH$_2$O - 18.2MΩ.cm) followed by a 90mM EDTA

158    wash, and then rinsed 3 times with ddH$_2$O. Restricted nutrient, iron-free media was prepared

159    modified from (34) as follows: 1L of ddH$_2$O mixed with 2g ammonium nitrate (Sigma-Aldrich, MO,

160    USA), 2g monobasic potassium phosphate (Merck, MA, USA), 0.5g magnesium sulphate

161    heptahydrate (Sigma-Aldrich, MO, USA), 0.1g calcium chloride (Bio Basics Canada Inc, ON,

162    Canada), 0.57mg boric acid (Sigma-Aldrich, MO, USA), 0.31mg zinc sulphate heptahydrate

163    (HIMEDIA labs, PA, USA), 0.039mg copper sulphate pentahydrate (Acros Organic, Belgium),

164    0.036mg manganese chloride tetrahydrate (Fisher Chemical), 0.018mg ammonium molybdate

165    tetrahydrate (Acros Organic, Belgium), and 0.001g thiamine HCl (Acros Organic, Belgium). For

166    carbon sources, glucose (Alpha Biosciences) 0.5% (w/v) and 50μm microcrystalline cellulose

167    (Acros Organics, Belgium) 1% (w/v) were used with five replicates for each culture and in each

168    medium. The media solution (200ml per 0.5L flask) was brought to a pH of 5.5 using NaOH and

169    autoclaved for 30 minutes. Liquid cultures were inoculated using mycelial slurries prepared by

170    scraping mycelium from fully grown agar plates into 50mL of sterile ddH$_2$O. One mL of mycelial

171    slurry was carefully pipetted onto the surface of the liquid media in each flask and allowed to

172    grow for six weeks to promote production of LMW metabolites.

173

174    **LMW metabolite extraction.** After incubation, inoculated liquid cultures were coarsely filtered

175    with Whatman #4 cellulose filters to remove the mycelium and cellulose microcrystals from the

176    liquid cultures, and this filtrate was then serially filtered through a 0.22μm cellulose filter under

177    vacuum. This was then followed by ultrafiltration through a 5kDa polyethersulfone filter used

178    with an Amicon Stirred Cell filtration unit (EMD Millipore, MA, USA) to yield the <5kDa LMW

179    metabolite fraction. A Bradford assay was conducted to confirm that proteins were not present

180    (results not shown). The LMW metabolite fraction was acidified to pH 3 with HCl prior to a triple

181    ethyl acetate (1:1 with ultrafiltered media) extraction for phenolics (33). The organic fraction was

182    dried under reduced pressure, resuspended in methanol, and filtered through a 0.22μm filter to

183    yield the final <5kDa LMW extract.

184

185 **Determination of total phenols by the Folin-Ciocalteu assay**. Folin-Ciocalteu (F-C) reagent

186 was used to spectrophotometrically quantify (765nm) the amount of total phenols in solution

187 (35) with gallic acid used as the standard. Samples of purified extract (20μl) and the F-C reagent

188 (100μl) were reacted (5min @RT) before the addition of 20% sodium carbonate (300μl) to initiate

189 the F-C reaction. After a further reaction period (2h @RT) in the dark, absorbance values were

190 compared to the gallic acid standard for phenolic concentration determination.

191

192 **Determination of iron reduction by Ferrozine assay**. The Ferrozine assay is a colorimetric

193 assay that is sensitive specifically to the ferrous form of iron and it is therefore useful in

194 measuring iron reduction capacity (36). Each reaction cuvette contained at their final

195 concentration: acetate buffer (0.100mM, pH 5.5), Ferrozine (0.250mM), $Fe^{3+}$ (0.030mM).

196 Phenolics in the fungal extract (15mM according to F-C assay) was added last to start the reaction.

197 Ferrous chloride ($FeCl_2$) was used for the standard. Samples were mixed thoroughly into each

198 cuvette and the reaction followed spectrophotometrically (562nm) at 5 min intervals for 45min.

199 The ferric iron reductive capacity of all LMW extracts was normalized per nmol of phenolics

200 added to the reaction and reported as the amount of iron reduced (mol)/amount of phenolic

201 (mol) in the extracts assayed.

202

203 **FOX assay for $H_2O_2$ detection.** A ferrous ammonium – xylenol orange (FOX) assay (37) was used

204 to measure $H_2O_2$ evolution which occurs during the oxidation of ferrous iron in Fenton chemistry.

205 The oxidized iron reacts with xylenol orange (XO) to form a blue purple complex that can be

206 detected at 560nm (37, 38). MES buffer (50mM, 5.5pH) and phenolics in fungal extracts (15mM

207   according to F-C assay) were added to 100μL of the FOX reagent (a 1:1 ratio of the XO/Ferrous

208   ammonium sulfate mixture and sorbitol) to yield a solution of 0.100mM XO, 0.250mM ferrous

209   ammonium sulfate, 25mM $H_2SO_4$, and 100mM sorbitol, which was incubated (RT, 30min) before

210   centrifugation (10,000RPM, 5min) to remove any precipitate. (Sorbitol was added consistently to

211   all samples to increase the yield of ferric iron). All samples were maintained in low light conditions

212   to reduce UV interference, analyzed at 560nm for $H_2O_2$ detection and reported as the amount of

213   $H_2O_2$ generated (mmol)/amount of phenolic (mol) in the extracts assayed.

214

215   **Electron paramagnetic resonance (EPR) for detection of hydroxyl radicals.** Methanol was

216   evaporated from each sample using a SpinVac (35ºC, 45min) after adding the fungal extract into

217   the reaction solvent at two pH values: (i) sodium acetate/acetic acid buffer (80mM, pH 5.5) and

218   (ii) acidified water (adjusted to pH 3.5 with $HNO_3$). For hydroxyl radical detection in EPR, the

219   following components (final concentration) were used in the reaction mixture:  DMPO spin-trap

220   (5,5-dimethyl-1-pyrroline-n-oxide, 10mM) was added to the other reaction components: $H_2O_2$

221   (0.15mM), phenolics in the fungal extract (50mM adjusted per the F-C assay). $Fe^{3+}$ (0.15mM) was

222   added to start the reaction, and after incubation (5 min, @RT) the samples were transferred to a

223   50μL EPR capillary glass tube. Catechol (50mM) was used as reference compound.  Analysis was

224   conducted in the X-band frequency (9.8 GHz) using a Bruker Elexsys-500 EPR instrument

225   equipped with a super high QE cavity (ER4122SHQE-W1).

226

227   **High performance liquid chromatography (HPLC).** LMW extracts were analyzed using a

228   Shimadzu HPLC system with an analytical C18 Nucleosil column (250mm x 4.6mm x 5μm,

10

229    0.50mL/min). Flow-through UV analysis (280nm) was conducted using an acetonitrile (ACN)

230    linear gradient (10-90%) over 45min. The gradient was then held at 90% for 5min and the gradient

231    reversed over the next 5 min before ending at 10% ACN over a total 60min. Fractions were then

232    scanned (190 – 370 nm) to detect potential phenolic compounds at ~280nm absorption.

233

234    **Identification of metabolites by ultra-performance liquid chromatography – mass spectroscopy**

235    **(UPLC-MS).** Fungal extracts were analyzed using an UPLC (ACQUITY HSS T3 (100×2.1mm×1.8μm)

236    with Ultimate 3000 LC) combined with a Q Exactive MS (Thermo) and screened with electrospray

237    ionization MS (ESI-MS). The mobile phase was: solvent A (0.05% formic acid water), and solvent

238    B (acetonitrile) with a gradient elution (0-1.0min, 5%B; 1.0-12.0min, 5%-95%B; 12.0-13.5min,

239    95%B; 13.5-13.6min, 95%-5%B; 13.6-16.0min, 5%B). The flow rate of the mobile phase was

240    0.3mL·min$^{-1}$ with the column temperature (40°C), and the sample manager (4°C), both constant.

241    Mass spectrometry parameters in ESI+ and ESI- mode were:

242    ESI+ : Heater Temp 300 °C; Sheath Gas Flow rate, 45arb; Aux Gas Flow Rate, 15arb; Sweep Gas

243    Flow Rate, 1arb; spray voltage, 3.0KV; Capillary Temp, 350 °C; S-Lens RF Level, 30%.

244    ESI- : Heater Temp 300 °C, Sheath Gas Flow rate, 45arb; Aux Gas Flow Rate, 15arb; Sweep Gas

245    Flow Rate, 1arb; spray voltage, 3.2KV; Capillary Temp,350 °C; S-Lens RF Level,60%.

246    Raw data was analyzed using Compound Discoverer$^{TM}$ (ThermoFisher Scientific) a high-resolution

247    accurate-mass data software for metabolite identification, and a comprehensive review was

11

248    conducted for each of the main compounds found in the extract selected by peak area or peak

249    height.

250

## RESULTS AND DISCUSSION

252

253    Cultures where two fungi were grown in consortia in some instances maintained a cultural

254    appearance that was characteristic of one of the species, and this always occurred when Pmin

255    was part of the consortia. With the Elata_Pch consortia growth, discrete colonies of both species

256    were apparent in about half the cultures whereas in the other half, Elata growth predominated.

257    However, when comparing the metabolomic profile of the individual cultures to the consortia

258    growth, unique extract profiles were observed in the consortia cultures as detailed below and in

259    Fig. S1.

260

261    **Production of phenolics and iron reduction capacity.** Preliminary chromatographic screening of

262    all fungal extracts by HPLC showed that putative phenolic compounds absorbing in the 280 nm

263    region were present (Fig. 1). All extracts contained a maximum of five detectable peaks absorbing

264    in the 280 nm range. Fig. 1 shows only the two most prominent phenolic peaks for extracts from

265    the three fungi.

266

267    The Folin-Ciocalteu (F-C) assay for phenolics in individual ~280nm UV fractions showed that Pch

268    extracts contained the largest amount of phenolics when compared to either the Elata or Pmin

269    individual fungal culture extracts (Table 1, $p < 0.001$, $p < 0.001$). Extracts from all fungal consortia

12

270     yielded an increase in total phenolics over individual cultures (Table 1). The Elata_Pmin consortia

271     produced significantly more phenolics than either Elata or Pmin alone (Table 1, p = 0.01, p = 0.03).

272     For the Elata_Pch consortia growth there was an averaging effect relative to phenolic production.

273     Phenolic content when Elata and Pch were grown in combination was significantly lower than

274     Pch alone (p < 0.001), but it was significantly higher than Elata alone (p = 0.007). The Pmin_Pch

275     combination showed an increase in overall phenolic production compared to that when the fungi

276     were grown individually. The additive effect alone may be an important finding relative to Eutypa

277     dieback and Esca.

278

279     Iron reduction was observed in all culture extracts. Elata and Pmin extracts both reduced

280     approximately the same level of iron per mol of phenols (0.531 and 0.615mol iron/mol of

281     phenolic). Pch extracts reduced more iron than the other two fungi per mol of phenolics (1.34mol

282     $Fe^{2+}$/mol of phenolic) reflecting the greater phenolic content (from the F-C results above). Pch

283     extracts also displayed a greater level of reduction per mol of phenolic, reducing more than

284     double the amount of iron compared to the extracts from Elata and Pmin in culture alone. The

285     Elata_Pmin combination showed a significantly increased level of iron reduction when compared

286     to each fungus by itself (p < 0.001, p = 0.001) but the reduction level was not great enough to be

287     considered an additive effect.  The combination of Pch_Pmin resulted in more limited total iron

288     reduction when compared to the extracts from each of the fungi when grown separately and

289     added together (p = 0.035, p = 0.005). Iron reduction in the Elata_Pch combined fungal cultures

290     was significantly greater than from Elata alone (p = 0.003), and the reduction level was

291     comparable to the Pch extracts when grown alone (p = 0.06).

13

292

293   **H$_2$O$_2$ production.** H$_2$O$_2$ is required in the CMF reaction to react with ferrous iron. Although some

294   enzymes are known to generate H$_2$O$_2$, enzymes are unable to penetrate intact plant cell walls

295   (18, 29, 39-43), and a catalytic source of H$_2$O$_2$ within the cell wall would promote a more efficient

296   CMF reaction.  Redox cycling of chelators with oxygen and transition metals in  acidic pH

297   environments is known to generate H$_2$O$_2$ in solution, thus promoting the production of hydroxyl

298   radicals (28), and we explored whether this mechanism might also be associated with the

299   phenolic components from the three fungi.

300

301   Extracts from Elata and Pmin produced the highest levels of H$_2$O$_2$ (690 and 800mmol H$_2$O$_2$/mol

302   of phenols) as determined by the FOX assay (Table 1). While Pch and all combinations had

303   detectable levels of H$_2$O$_2$ generation, they were in the 0.4 to 9mmol range and significantly lower

304   than both Elata and Pmin (Pch vs Elata: p = 0.006, Pch vs Pmin: p < 0.001, Elata vs Pch_Elata: p =

305   0.006, Pmin vs Pch_Pmin: p = 0.005). Based on the results from the F-C and Ferrozine assay, it

306   was expected that the Elata_Pmin combination extract would show higher levels of H$_2$O$_2$

307   production than Elata and Pmin extracts. However, H$_2$O$_2$ production in extracts from this

308   combination was below 10 mmol, and although still significantly higher than the Pch extract alone

309   (p < 0.001) it was well below the 690 and 800mmol levels seen for the individual cultures of Elata

310   and Pmin respectively. This may be due to the metabolite profile for the combined culture of

311   Elata and Pmin being distinct from the individual cultures and lacking in the primary metabolites

312   seen in the cultures when grown alone (See "Identification of LMW Metabolites" section below).

313 **TABLE 1** Total phenolic content (Folin-Ciocalteu) of LMW fungal extracts from the three GTD
314 fungi, together with iron reduction (Ferrozine), and $H_2O_2$ production (FOX) from those extracts.
315 Results shown as mean ± SD, n = 3.

| | Total phenolic content (mM) | Iron reduced (mol $Fe^{2+}$/mol of phenols) | $H_2O_2$ produced (mmol $H_2O_2$/per mol phenols) |
|---|---|---|---|
| Elata | 1.03 ± 0.08 | 0.531 ± 0.010 | 690 ± 70 |
| Pmin | 1.07 ± 0.10 | 0.615 ± 0.013 | 800 ± 20 |
| Pch | 3.33 ± 0.36 | 1.34 ± 0.08 | 1.6 ± 0.1 |
| Elata_Pmin | 1.22 ± 0.107 | 0.877 ± 0.026 | 8.8 ± 0.3 |
| Elata_Pch | 2.25 ± 0.25 | 1.16 ± 0.05 | 1.7 ± 0.2 |
| Pmin_Pch | 4.05 ± 0.20 | 1.62 ± 0.10 | 0.4 ± 0.1 |

316

317

318 **Electron Paramagnetic Resonance (EPR).** A DMPO-HO$^\bullet$ adduct with its characteristic 4-line

319 spectrum allowed detection and quantification of HO$^\bullet$ in solution (Fig. 2). All extracts were found

320 to generate HO$^\bullet$ when examined in the EPR studies for radical generation for pH values of both

321 3.5 and 5.5. The production of HO$^\bullet$ was considerably greater at pH 3.5 for most of the treatments

322 tested. It should be noted that only cultures containing Pch reached pH 3-3.5 under the

323 experimental conditions tested. Uniquely, all extracts produced more HO$^\bullet$ than a reference

324 catechol compound at the same concentration based on F-C analysis of phenolics. Catechol is

325 typically used as a standard in iron-reduction assays because of its capacity for iron reduction

326 (44).

327

328

15

329   **Identification of LMW metabolites.** Metabolite identification analysis of the three fungi in

330   individual cultures (Fig. S2-S4) showed that several phenolic and non-phenolic compounds were

331   present, with some of them previously reported as having iron reduction capacity (Table 2).

332   Interestingly, all fungi produced small catecholates like 3,4-dihydroxybenzoic acid (Elata), caffeic

333   acid (Pmin) and hydroxycinnamic acids like sinapinic acid (Pch, Pmin) and caffeic acid (Pmin).

334   Catecholates and hydroxycinnamic acids chelate iron and are known for their ability to increase

335   the production of ROS under appropriate conditions (44-46)**.** In addition, Elata also produces

336   pyochelin, a phenolic siderophore and iron reducing compound that is one of the primary

337   siderophores isolated from *Pseudomonas spp.*; and terrein, a non-phenolic iron reducer also

338   found in *Aspergillus terreus* with reported anticarcinogenic activity (47).

339

340   MS analysis also identified other organic phenols, aldehydes, and carboxylic acids (Table 3)

341   without previously reported iron reduction activity; however, some structures suggest that they

342   could potentially chelate iron. Further experiments with individual model metabolites would be

343   required to demonstrate this, however.

344

345   **TABLE 2** Metabolites produced by *E. lata*, *P. minimum*, and *P. chlamydospora* with previously
346   reported capacity for iron reduction.

| Compound | Formula | Elata | Pmin | Pch | Ref |
|---|---|---|---|---|---|
| Pyochelin | $C_{14}H_{16}N_2O_3S_2$ | ● | | | (48) |
| 3,4-dihydroxybenzoic acid | $C_7H_6O_4$ | ● | | | (49) |
| Terrein | $C_8H_{10}O_3$ | ● | | | (50) |
| Sinapic acid methyl ester | $C_{12}H_{14}O_5$ | | ● | ● | (51) |
| Dihydroferulic acid | $C_{10}H_{12}O_4$ | | | ● | (52) |
| Caffeic acid | $C_9H_8O_4$ | | ● | | (53) |

16
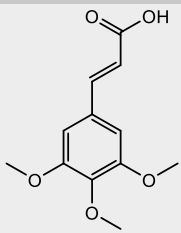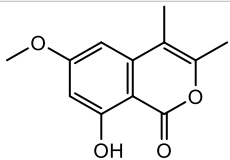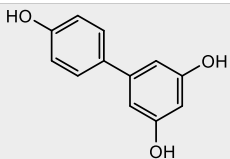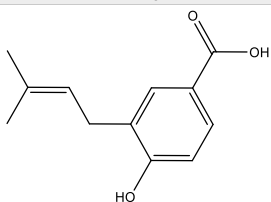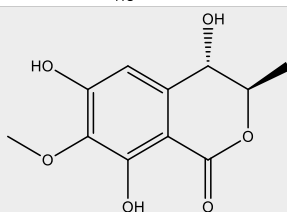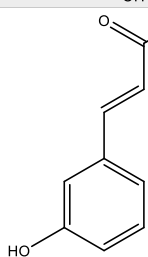
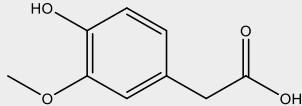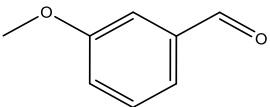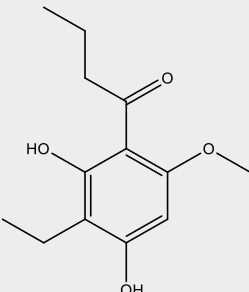| Gallic acid | $C_7H_6O_5$ | | ● | | (54) |
| Homogentisic acid | $C_8H_8O_4$ | | ● | | (55) |
| Sinapinic acid | $C_{11}H_{12}O_5$ | | ● | | (56) |

347

348

349 **TABLE 3** Mass Spectral analysis of phenolic, aldehydes, and carboxylic acid metabolites produced
350 by *E. lata*, *P. minimum*, and *P. chlamydospore* without reported iron reduction activity.
351

| Compound | Formula | Structure | Elata | Pmin | Pch |
|---|---|---|---|---|---|
| 3,4,5-trimethoxycinnamic acid | $C_{12}H_{14}O_5$ |  | ● | | |
| Polygonolide | $C_{12}H_{12}O_4$ |  | ● | | |
| 3,4',5-Biphenyltriol | $C_{12}H_{10}O_3$ |  | ● | | |
| 4-hydroxy-3-(3-methylbut-2-enyl)benzoic acid | $C_{12}H_{14}O_3$ |  | | ● | ● |
| 4,6,8-trihydroxy-7-methoxy-3-methyl-3,4-dihydroisochromen-1-one (Lignicol) | $C_{11}H_{12}O_6$ |  | | ● | |
| 3-coumaric acid | $C_9H_8O_3$ |  | | | ● |

| Homovanillic acid | $C_9H_{10}O_4$ |  | | | ● |
| 3-Methoxybenzaldehyde | $C_8H_8O_2$ |  | | | ● |
| 1-(3-ethyl-2,4-dihydroxy-6-methoxyphenyl)butan-1-one (Deoxyphomalone) | $C_{13}H_{18}O_4$ |  | | | ● |

352

353

354 Based on our findings from both the iron reduction and hydrogen peroxide production analyses,

355 we propose that some GTD fungi produce LMW metabolites that are responsible for iron

356 reduction, while other fungi produce LMW metabolites that play a greater role in hydrogen

357 peroxide/oxidant production (Table 1). The LMW extracts from Elata and Pmin possessed

358 relatively limited iron-reduction capacity but produced a significantly greater amount of

359 hydrogen peroxide than Pch. Extracts from the fungal consortia combinations possessed iron

360 reduction capability, but virtually no hydrogen peroxide was observed, including in the

361 combination Elata Pmin. Our MS analysis (Table 2) showed at least five metabolites with iron

362 reduction capacity were identified from Pmin; with Elata and Pch producing 3 and 2 iron reducing

363 metabolites, respectively. We suggest that individual fungi in GTD consortia produce LMW

364 metabolites with specialized and differential functions, with some species taking on greater roles

365 in the production of iron-reducing metabolites while other species produce metabolites with

366 greater capacity for peroxide generation. This may help to explain why GTD pathogenesis is often

367 associated with a consortium of GTD fungi rather than individual fungi.

368

369 As detailed in the CMF mechanism for brown rot fungi (19), we proposed that $H_2O_2$ reacts with

370 reduced iron to allow targeted ROS generation such as hydroxyl radicals within plant/wood cell

371 walls to initiate digestion of the lignocellulose components (as part of pathogenesis). In the case

372 of Eutypa dieback and the Esca disease complex, for wood necrosis to occur by a similar

373 mechanism these reactions would also need to occur in tissue that is maintained at a pH $\leq$ 5.5.

374 This falls into the range of the natural pH of wood cell walls, and our results also show that a pH

375 of ~5.5 was maintained by individual liquid cultures of Pmin and Elata throughout the growth

376 period of 6 weeks (data not shown). However, in Pch cultures (grown either alone, or in

377 combination with either Pmin or Elata) the pH dropped to 3-3.5. The reduction in pH by Pch may

378 also help explain why different consortia fungi are required in GTD pathogenesis, as pH

379 modification potentially changes the fungal/wood micro-environment to promote the select

380 oxidative chemistries that we report here. Similar oxidative chemistries have also been observed

381 with other catecholate fungal metabolites (19, 25). It has been demonstrated that acidic

382 environments enhance iron reduction by phenolic compounds, and this is observed in our

383 ferrozine assay results (Table 1) where extracts from Pch alone or in consortia reduced more iron

384 than any other fungal extract produced from either individual fungi or consortia growth. The

385 reduction in pH by Pch alone, or in consortia, supports the hypothesis that GTD fungal consortia

386 are necessary for reduction of pH to promote iron reduction as a precursor to the generation of

387 damaging hydroxyl radical generation. This, together with the differential promotion of CMF

388    chemistry by different fungal metabolites, is a novel concept relative to pathogenesis

389    mechanisms associated with consortia fungal activity and grapevine trunk disease that has not

390    previously been reported.

391

392    Further exploration of this mechanism could potentially open new alternatives for treatments to

393    prevent or limit yield loss in vineyards. Fig. 3 summarizes our hypothesized mechanism for the

394    initiation of the wood cell wall damage by GTD fungi through $HO^{\bullet}$ generation by LMW metabolite

395    secretion. Lignin depolymerization via this LMW mechanism would promote lignocellulose cell

396    wall damage to produce features of necrosis, and after the initiation of this degradation, would

397    potentially allow extracellular fungal CAZymes to further depolymerize the wood cell wall. In later

398    stages, as vine defenses are overwhelmed, the fungal LMW metabolites would also potentially

399    be transported via the vascular system of the stem to promote further necrosis of cordon wood

400    and ultimately leaf tissue with disease progression.

401

402

403    **CONCLUSIONS**
404

405    Our data indicates that some GTD fungi preferentially promote iron reduction in culture, while

406    others boost $H_2O_2$ production, suggesting that a mechanism similar to the CMF mechanism

407    employed by brown rot fungi in wood biodegradation may also play a role in GTD pathogenesis.

408    Since both iron reduction and $H_2O_2$ production are required in CMF systems for generation of

409    hydroxyl radicals, this may help to explain why GTDs are often caused by a consortium of fungi

410    rather than individual species. Often these diseases are associated with what has been described

20

411 previously as non-causative fungi, but the role of LMW in GTD Eutypa and Esca pathogenesis has

412 not been well explored. Our observation of differential function of extracellular LMW metabolites

413 from GTD consortia fungi has not previously been reported, even in brown rot Basidiomycota

414 species where the role of LMW metabolites in wood decay has been established. Thus, this is the

415 first report of the differential action of LMW metabolites promoting the sequential steps of a

416 mediated Fenton chemistry related to pathogenesis in grapevine tissue. We also observed that

417 one fungus in the consortium promoted establishment of a lower pH environment. Pch reduced

418 the pH of the media to 3-4 when grown alone in cultures, but also in consortia with either Elata

419 or Pmin. This pH promotes iron reduction by catecholates, and our observation that Pch reduces

420 pH of the media, while Elata/Pmin maintain pH constant (5.5), may also help to explain why

421 fungal consortia growth is required in many GTDs. Additional research must be conducted to

422 isolate individual LMW metabolites to determine their specific role in GTD fungal consortia ;

423 however, our MS analysis has already identified select metabolites from each of the three fungal

424 species studied which have previously been reported to possess iron-reduction capability. Future

425 research will assess whether these specific LMW metabolites also aid in promoting CMF

426 chemistry and the generation of hydroxyl radicals as a component of pathogenesis.

427

428

433    *chalmydospora*, *Phaeacremonium minimum* and *Eutypa lata* used in this study.  We appreciate

434    the support of Professor Kevin Kittilstved from the Department of Chemistry at the University of

435    Massachusetts, Amherst, in allowing the use of their EPR facilities. Mass Spectral analysis was

436    conducted by Creative biolabs (Shirley, NY).

443    **AUTHOR CONTRIBUTIONS**

444

445     Conceptualization, Barry Goodell; Methodology, Dana Sebestyen, Gabriel Perez-Gonzalez and

446    Barry Goodell; Validation, Barry Goodell; Formal Analysis, Dana Sebestyen, Gabriel Perez-

447    Gonzalez, Norman Lee; Investigation, Dana Sebestyen and Gabriel Perez-Gonzalez.; Resources,

448    Barry Goodell and Christophe Bertsch.; Writing – Original Draft Preparation, Dana Sebestyen and

449    Gabriel Perez-Gonzalez; Writing – Review & Editing, Dana Sebestyen, Gabriel Perez-Gonzalez,

450    Elsa Petit, Jody Jellison, Laura Mugnai, Christophe Bertsch,  Sibylle Farine, Eric Gelhaye, and Barry

451    Goodell; Visualization, Barry Goodell, Dana Sebestyen and Gabriel Perez-Gonzalez; Supervision,

452    Barry Goodell, Gabriel Perez-Gonzalez, Jody Jellison, Elsa Petit; Project Administration, Barry

453    Goodell.; Funding Acquisition, Barry Goodell.

454

## REFERENCES

1.	Surico G, Mugnai L, Marchi G. Older and more recent observations on esca: a critical overview. Phytopathologia Mediterranea 2006;45:S68-S86.
2.	Bertsch C, Larignon P, Farine S, Clément C, Fontaine F. The Spread of Grapevine Trunk Disease. Science. 2009;324:721-.
3.	Bertsch C*ea*. Grapevine trunk diseases: complex and still poorly understood. Plant Pathology 2013;62:243-65.
4.	Labois C, Wilhelm K, Laloue H, Tarnus C, Bertsch C, Goddard M-L, et al. Wood Metabolomic Responses of Wild and Cultivated Grapevine to Infection with Neofusicoccum parvum, a Trunk Disease Pathogen. Metabolites. 2020;10(6):232.
5.	Mondello V, Songy A, Battiston E, Pinto C, Coppin C, Trotel-Aziz P, et al. Grapevine Trunk Diseases: A Review of Fifteen Years of Trials for Their Control with Chemicals and Biocontrol Agents. Plant Disease. 2018;102(7):1189-217.
6.	Berraf-Tebbal A, Bouznad Z, Santos JM, Coelho M, Peros JP, Phillips AJL. Phaeoacremonium species associated with Eutypa dieback and esca of Grapevines in Algeria. Phytopathologia Mediterranea. 2011;50 86-97.
7.	Rolshausen PE, Baumgartner K, Travadon R, Fujiyoshi P, Pouzoulet J, Wilcox WF. Identification of Eutypa spp. Causing Eutypa Dieback of Grapevine in Eastern North America. Plant Disease. 2013;98(4):483-91.
8.	Morales-Cruz A, Figueroa-Balderas R, García JF, Tran E, Rolshausen PE, Baumgartner K, et al. Profiling grapevine trunk pathogens in planta: a case for community-targeted DNA metabarcoding. BMC Microbiology. 2018;18(1):214.
9.	Bruez E, Lecomte P, Grosman J, Doublet B, Bertsch C, Fontaine F, et al. Overview of grapevine trunk diseases in France in the 2000s Phytopathologia Mediterranea. 2013;52(2):262-75.
10.	Fontaine F*ea*. Grapevine Trunk Diseases: A Review. International Organization of Vine and Wine Intergovernmental Organization. 2016.
11.	Siebert J. Eutypa: The economic toll on vineyards. Wines Vines April 2001:50-6.
12.	Hofstetter v, Buyck B, Croll D, Viret O, Couloux A, Gindro K. What if esca disease of grapevine were not a fungal disease? Fungal Diversity. 2012;54:51-67.
13.	Tey-Rulh P, Philippe I, Renaud J-M, Tsoupras G, de Angelis P, Fallot J, et al. Eutypine, a phytotoxin produced by Eutypa lata the causal agent of dying-arm disease of grapevine. Phytochemistry. 1991;30(2):471-3.
14.	Claverie M, Notaro M, Fontaine F, Wery J. Current knowledge of Grapevine Trunk Diseases with complex etiology: a systemic approach. Phytopathologia Mediterranea. 2020;59(1):29-53.
15.	Xu G, Goodell B. Mechanisms of wood degradation by brown-rot fungi: chelator-mediated cellulose degradation and binding of iron by cellulose. Journal of Biotechnology. 2001;87(1):43-57.
16.	Goodell B. Brown-Rot Fungal Degradation of Wood: Our Evolving View. Wood Deterioration and Preservation. 2003;845:97-118.
17.	Goodell B, Qian Y, Jellison J. Fungal Decay of Wood: Soft Rot-Brown Rot-White Rot. Development of Commerical Wood Preservatives. 2008;982.
18.	Arantes V, Jellison J, Goodell B. Peculiarities of brown-rot fungi and biochemical Fenton reaction with regard to their potential as a model for bioprocessing biomass. Applied Microbiology and Biotechnology 2012;94:323-38.
19.	Goodell B. Fungi Involved in the Biodeterioration and Bioconversion of Lignocellulose Substrates. In: Benz JP, Schipper K, editors. Genetics and Biotechnology. . 2. The Mycota (A

23

501 Comprehensive Treatise on Fungi as Experimental Systems for Basic and Applied Reasearch) Chapter
502 15.: Springer, Cham; 2020. p. 369-97.
503 20. Hess J, Balasundaram SV, Bakkemo RI, Drula E, Henrissat B, Högberg N, et al. Niche
504 differentiation and evolution of the wood decay machinery in the invasive fungus Serpula lacrymans.
505 The ISME Journal DOI 101038/s41396-020-00799-5. 2020.
506 21. Kent MS, Zeng J, Rader N, Avina IC, Simoes CT, Brenden CK, et al. Efficient conversion of lignin
507 into a water-soluble polymer by a chelator-mediated Fenton reaction: optimization of H2O2 use and
508 performance as a dispersant. Green Chemistry. 2018;20(13):3024-37.
509 22. Goodell B, Zhu Y, Kim S, Kafle K, Eastwood D, Daniel G, et al. Modification of the nanostructure
510 of lignocellulose cell walls via a non-enzymatic lignocellulose deconstruction system in brown rot wood-
511 decay fungi. Biotechnology for Biofuels. 2017;10.
512 23. Rolshausen PE, Greve LC, Labavitch JM, Mahoney NE, Molyneux RJ, Gubler WD. Pathogenesis of
513 Eutypa lata in Grapevine: Identification of Virulence Factors and Biochemical Characterization of Cordon
514 Dieback. Phytopathology®. 2008;98(2):222-9.
515 24. Osti F, Di Marco S. Iron-dependent, non-enzymatic processes promoted by Phaeomoniella
516 chlamydospora and Phaeoacremonium aleophilum, agents of esca in grapevine. Physiological and
517 Molecular Plant Pathology. 2010;74:309-16.
518 25. Goodell B*ea*. Low molecular weight chelators and phenolic compounds isolated from wood
519 decay fungi and their role in the fungal biodegradation of wood. Journal of Biotechnology. 1997;53:133-
520 62.
521 26. Contreras D, Rodríguez J, Freer J, Schwederski B, Kaim W. Enhanced hydroxyl radical production
522 by dihydroxybenzene-driven Fenton reactions: implications for wood biodegradation. JBIC Journal of
523 Biological Inorganic Chemistry. 2007;12(7):1055-61.
524 27. Varela E, M T. Effect of pH and oxalate on hyroquinone-derived hydroxyl radical formation
525 during brown rot wood degradation. Applied and Environmental Microbiology. 2003;69(10):6025-31.
526 28. Akagawa M, Shigemitsu T, Suyama K. Production of Hydrogen Peroxide by Polyphenols and
527 Polyphenol-rich Beverages under Quasi-physiological Conditions. Bioscience, Biotechnology, and
528 Biochemistry. 2003;67(12):2632-40.
529 29. Zhu Y, Liu J, Wang C, Goodell B, Esker A. Chelator-mediated biomimetic degradation of cellulose
530 and chitin. International Journal of Biological Macromolecules. 2020;153:433-40.
531 30. Mahoney N, Lardner R, Molyneux R, Scott E, Smith L, Schoch T. Phenolic and heterocyclic
532 metabolite profiles of the grapevine pathogen Eutypa lata. Phytochemistry. 2003;64(2):475-84.
533 31. Molyneux R, Mahoney N, Bayman P, Wong R, Meyer K, Irelan N. Eutypa Dieback in Grapevines:
534 Differential Production of Acetylenic Phenol Metabolites by Strains of Eutypa lata. Journal of Agricultural
535 and Food Chemistry. 2002;50(6):1393-9.
536 32. Andolfi A, Mugnai L, Luque J, Surico G, Cimmino A, Evidente A. Phytotoxins Produced by Fungi
537 Associated with Grapevine Trunk Diseases. Toxins. 2011;3(12):1569-605.
538 33. Jellison J, Chandhoke V, Goodell B, Fekete FA. The isolation and immunolocalization of iron-
539 binding compounds produced by *Gloeophyllum trabeum*. Applied Microbiology and Biotechnology.
540 1991;35:805-9.
541 34. Highley T. Influence of carbon source on cellulase activity of white-rot and brown-rot fungi.
542 Wood and Fiber. 1973;5(1).
543 35. Singleton V, Orthofer R, Lamueala-Raventos R. Analysis of total phenols and other oxidation
544 substrates and antioxidants by means of folin-ciocalteu reagent. Methods in Enzymology. 1999;299:152-
545 78.
546 36. Pierson EE, Clark RB. Ferrous Iron Determination in Plant Tisue. Journal of Plant Nutrition.
547 1984;7:107-16.

548  37.    Wolff S. Ferrous ion oxidation in presence of ferric ion indicator xylenol orange for
549  measurement of hydroperoxides. Methods in Enzymology. 1994;233:182-9.
550  38.    Rhee SG, Chang T-S, Jeong W, Kang D. Methods for Detection and Measurement of Hydrogen
551  Peroxide Inside and Outside of Cells. Molecules and Cells. 2010;29:539-49.
552  39.    Goodell B*ea*. Modification of the nanostructure of lignocellulose cell walls via a non-enzymatic
553  lignocellulose deconstruction system in brown rot wood-decay fungi. Biotechnology for Biofuels
554  2017;10.
555  40.    Tepfer M, Taylor IEP. The interaction of divalent cations with pectic substances and their
556  influence on acid-induced cell wall loosening. Canadian Journal of Botany. 1981;59(8):1522-5.
557  41.    Flournoy DS, Kirk TK, Highley TL. Wood decay by brown-rot fungi : changes in pore structure and
558  cell wall volume. Holzforschung. 1991;45:383-8.
559  42.    Kleman-Leyer K, Agosin E, Conner AH, Kirk TK. Changes in Molecular Size Distribution of
560  Cellulose during Attack by White Rot and Brown Rot Fungi. Applied and Environmental Microbiology.
561  1992;58(4):1266-70.
562  43.    Cragg SM, Beckham GT, Bruce NC, Bugg TDH, Distel DL, Dupree P, et al. Lignocellulose
563  degradation mechanisms across the Tree of Life. Current Opinion in Chemical Biology. 2015;29:108-19.
564  44.    Tamaru Y, Yoshida M, D. Eltis L, Goodell B. Multiple iron reduction by methoxylated phenolic
565  lignin structures and the generation of reactive oxygen species by lignocellulose surfaces. International
566  Journal of Biological Macromolecules. 2019;128:340-6.
567  45.    Maurya DK, Devasagayam TPA. Antioxidant and prooxidant nature of hydroxycinnamic acid
568  derivatives ferulic and caffeic acids. Food and Chemical Toxicology. 2010;48(12):3369-73.
569  46.    Salgado P, Melin V, Contreras D, Moreno Y, Mansilla HD. Fenton reaction driven by iron ligands.
570  Journal of the Chilean Chemical Society. 2013;58:2096-101.
571  47.    Asfour HZ, Awan ZA, Bagalagel AA, Elfaky MA, Abdelhameed RFA, Elhady SS. Large-Scale
572  Production of Bioactive Terrein by Aspergillus terreus Strain S020 Isolated from the Saudi Coast of the
573  Red Sea. Biomolecules. 2019;9(9):480.
574  48.    Coffman TJ, Cox CD, Edeker BL, Britigan BE. Possible role of bacterial siderophores in
575  inflammation. Iron bound to the Pseudomonas siderophore pyochelin can function as a hydroxyl radical
576  catalyst. The Journal of Clinical Investigation. 1990;86(4):1030-7.
577  49.    Spiegel M, Kapusta K, Kołodziejczyk W, Saloni J, Żbikowska B, Hill GA, et al. Antioxidant Activity
578  of Selected Phenolic Acids-Ferric Reducing Antioxidant Power Assay and QSAR Analysis of the Structural
579  Features. Molecules (Basel, Switzerland). 2020;25(13):3088.
580  50.    Gressler M, Meyer F, Heine D, Hortschanksy P, Hertweck C, Brock M. Phytotoxin production in
581  *Aspergillus terreus* is regulated by independent environmental signals. Biochemistry and Chemical
582  Biology, Microbiology and Infecious diseases. 2015.
583  51.    Siger A, Czubinski J, Dwiecki K, Kachlicki P, Nogala-Kalucka M. Identification and antioxidant
584  activity of sinapic acid derivatives in Brassica napus L. seed meal extracts. European Journal of Lipid
585  Science and Technology. 2013;115(10):1130-8.
586  52.    Chen H, Virk MS, Chen F. Phenolic acids inhibit the formation of advanced glycation end
587  products in food simulation systems depending on their reducing powers and structures. International
588  Journal of Food Sciences and Nutrition. 2016;67(4):400-11.
589  53.    Gülçin İ. Antioxidant activity of caffeic acid (3,4-dihydroxycinnamic acid). Toxicology.
590  2006;217(2):213-20.
591  54.    Powell H, Taylor M. Interactions of iron(II) and iron(III) with gallic acid and its homologues: a
592  potentiometric and spectrophotometric study. Australian Journal of Chemistry. 1982;35(4):739-56.
593  55.    Martin JP, Batkoff B. Homogentisic acid autoxidation and oxygen radical generation: implications
594  for the etiology of alkaptonuric arthritis. Free Radical Biology and Medicine. 1987;3(4):241-50.

595    56.    Hynes MJ, O'Coinceanainn Mn. The kinetics and mechanisms of reactions of iron(III) with caffeic
596    acid, chlorogenic acid, sinapic acid, ferulic acid and naringin. Journal of Inorganic Biochemistry.
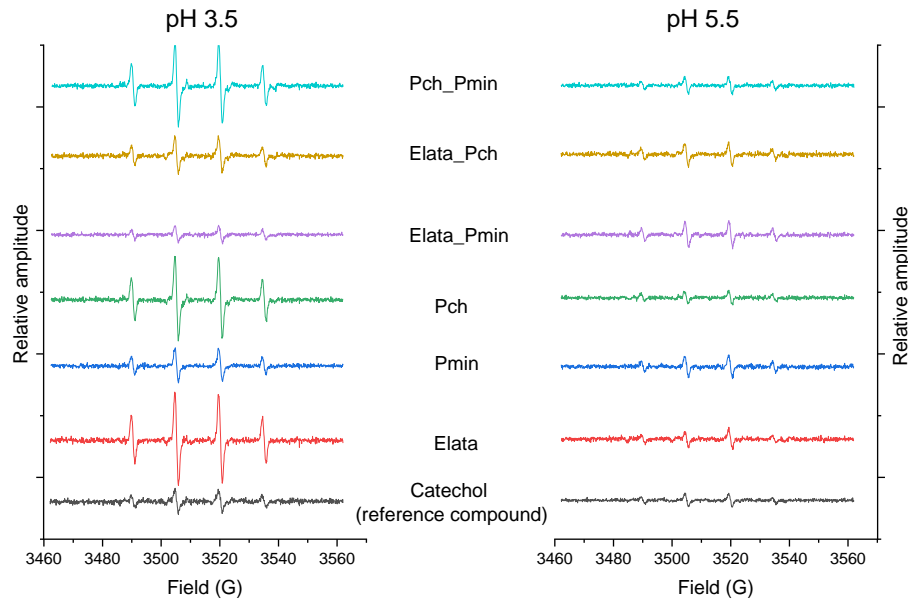597    2004;98(8):1457-64.

598

599

600
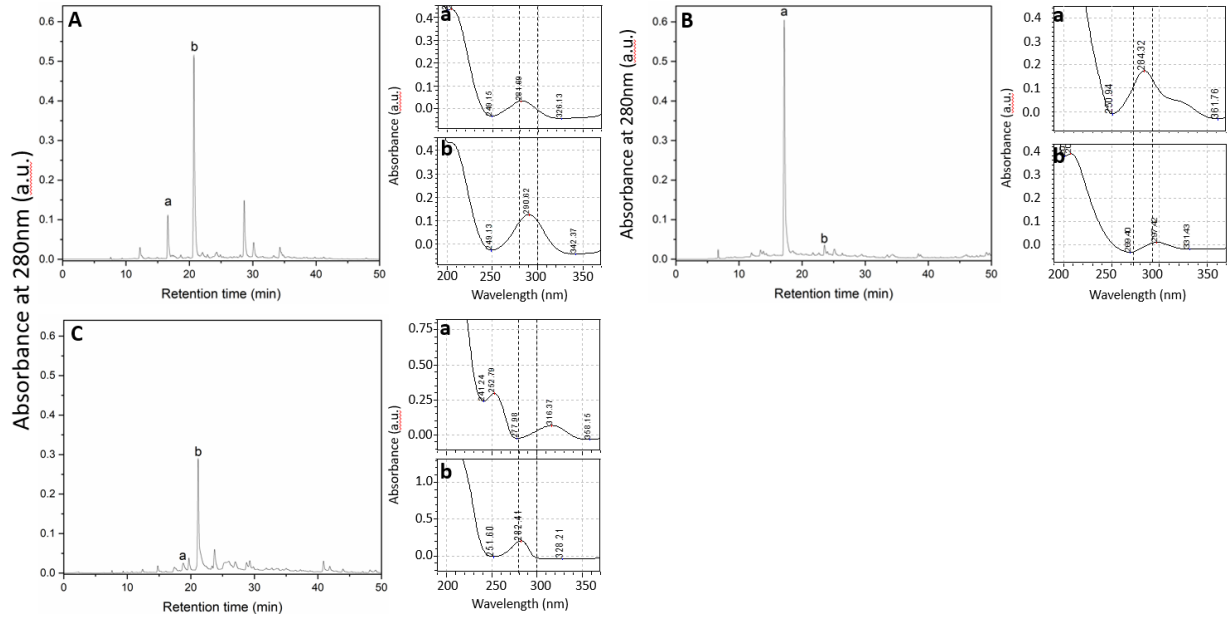


**FIG 1** HPLC chromatograms (Left for each sample) of (A) Elata, (B) Pmin, and (C) Pch fungal metabolite extracts taken at 280nm. Labels (a,b) indicate the putative phenolic peaks selected (abs. ~280nm). (Right) UV spectra of the two most abundant extract peaks.

604



605

**FIG 2** Electron paramagnetic resonance (EPR) spectra of GTD fungal extracts spiked with DMPO to detect hydroxyl radicals. The relative amplitude of each 4-peak spectra reflects the amount of hydroxyl radical produced relative to a catechol standard. Fungi were grown alone, and in consortia, to produce the extracts analyzed in this work.
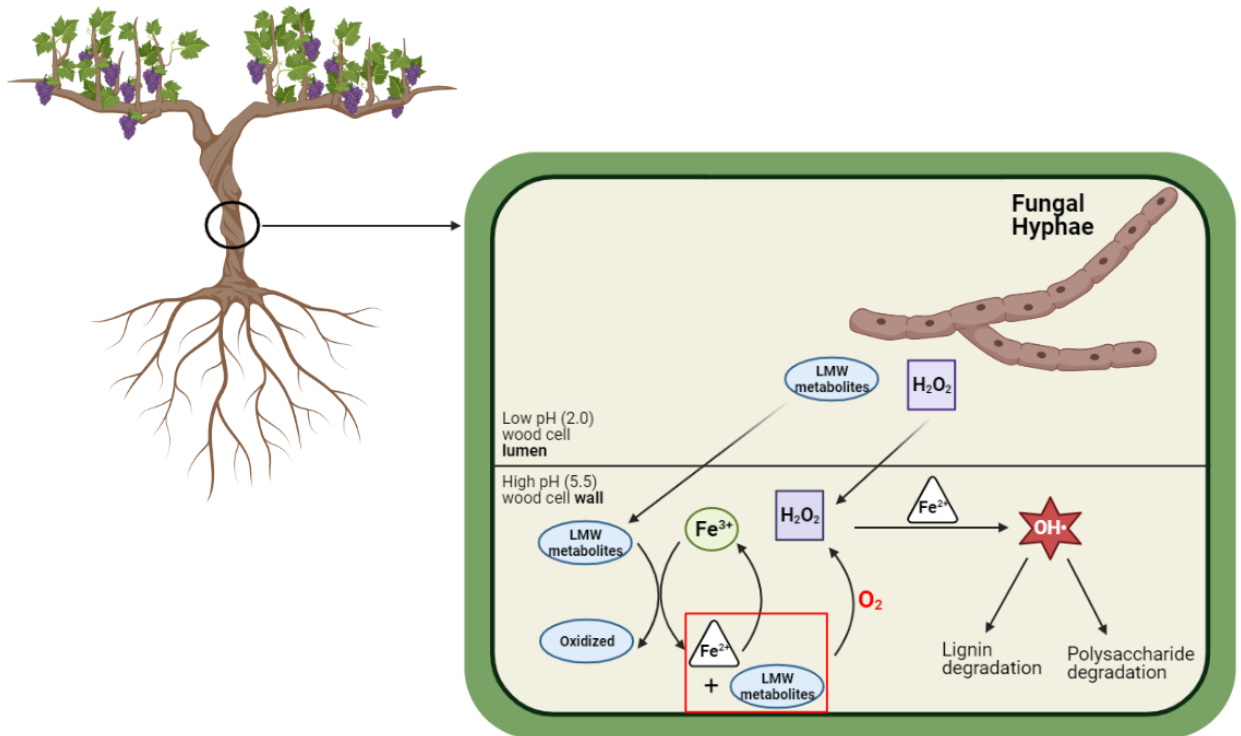
610

611 **FIG 3** Mechanism for the in-situ generation of $Fe^{2+}$ and $H_2O_2$, and degradation of lignin and cell
612 wall macromolecules by GTD fungi. LMW metabolites and $H_2O_2$ diffuse into the cell wall, where
613 the LMW metabolites sequester $Fe^{3+}$ from the cell wall environment and reduce $Fe^{3+}$ to $Fe^{2+}$.
614 Through the mediated Fenton reaction, $Fe^{2+}$ and $H_2O_2$ react and generate hydroxyl radicals ($OH^•$).
615 Images built using Biorender software. Schematic modified from (29).

616